O_2-coverage-dependent CO oxidation on reduced TiO_2(110): A first principles study

Devina Pillay and Gyeong S. Hwang[a)]
Department of Chemical Engineering, The University of Texas at Austin, Austin, Texas 78712-0231

(Received 30 May 2006; accepted 16 August 2006; published online 11 October 2006)

First principles periodic slab calculations based on gradient-corrected density functional theory have been performed to investigate CO oxidation on rutile TiO_2(110) at varying O_2 coverages (θ=1, 2, and 3, where θ is defined as the number of O_2 per oxygen vacancy). For each coverage we only present the reaction of CO with oxygen species in the most stable configuration. Our results show a significant variation in the oxidation activation energy with O_2 coverage. © *2006 American Institute of Physics*. [DOI: 10.1063/1.2354083]

I. INTRODUCTION

The rutile TiO_2(110) is one of the most studied oxide surfaces due to its important technological applications in photocatalysis,[1] gas sensing,[2] and heterogeneous catalysis.[3–5] The rutile surface has also been widely chosen as a prototype system for studies of fundamental chemical and physical phenomena occurring on oxide surfaces. The TiO_2 surface usually contains a high density of surface defects, mostly oxygen vacancies at protruding oxygen rows. Apart from the defects, molecularly adsorbed oxygen has a strong influence on the electronic structure and the chemical reactivity of TiO_2 surfaces. Earlier temperature programed desorption (TPD) measurements have shown that each vacancy could be responsible for the binding of three O_2 molecules at saturation coverage.[6] However, the atomic structure and reactivity of adsorbed oxygen species at varying O_2 coverages are still uncertain. In this paper, we focus on the effect of varying O_2 coverage on the CO oxidation reaction on TiO_2(110).

Thermally activated oxidation of CO on O_2-predosed TiO_2(110) samples at room temperature has recently been identified from TPD experiments by Lee *et al.*[7] In addition, Yates and co-workers[8,9] determined the existence of two distinct chemisorption states for molecular oxygen on TiO_2(110); that is, one (α state) can photo-oxidize coadsorbed CO and the other (β state) only undergoes fast photodesorption. While the reactivity change is associated with the various states of adsorbed oxygen species, the exact adsorption configurations and reaction mechanisms are not clearly understood. In fact, recent first principles studies have mainly focused on understanding the nature of O_2 interaction with the reduced surface by examining the adsorption and dissociation of a single oxygen molecule per vacancy or more[10–12] as well as the reaction of CO with molecularly adsorbed O_2 at the oxygen vacancy site.[13] To our best knowledge, no theoretical calculation has been undertaken to examine how the variation in O_2 coverage influences the chemical reactivity of adsorbed oxygen species and TiO_2(110) surfaces.

In this article, based on gradient-corrected density functional calculations we present the lowest-energy atomic configurations of adsorbed oxygen species at varying O_2 coverages, the adsorption properties of CO, and the pathways and barriers for O_2-coverage-dependent CO oxidation reactions. Results from our first principles study of the coverage-dependent behavior will greatly assist in understanding and predicting complex oxidation processes occurring on TiO_2(110).

II. COMPUTATION METHODS

All atomic structures and energies reported herein were calculated within the generalized gradient approximation[14] (PW91) to spin-polarized density functional theory (DFT) using the well-established Vienna *ab initio* simulation package (VASP).[15] A plane-wave basis set for valence electron states and Vanderbilt ultrasoft pseudopotentials for core-electron interactions were employed. We used a plane-wave cutoff energy of 300 eV and a $(2\times4\times1)$ Monkhorst-Pack mesh of k points to sample the Brillouin zone for a (2×3) surface unit cell. The TiO_2(110) surface is modeled using a 15-atomic-layer (2×3) slab that is separated from its periodic images by a vacuum space of 10 Å. Here, three atomic layers correspond to one O–Ti–O layer which has also been commonly adopted in literature. All adsorbates and Ti/O atoms in the top nine atomic layers were fully relaxed using the conjugate gradient method until residual forces on the relaxed atoms become smaller than 5×10^{-2} eV/Å. The chosen parameters have been proven to be sufficient for describing the Au–TiO_2(110) system.[16–19] We used the nudged elastic band method (NEBM) with eight intermediate images in the search of diffusion pathways and barriers.[20]

III. RESULTS AND DISCUSSION

Figure 1(a) shows a schematic of the stoichiometric TiO_2(110) surface which consists of two types of Ti atoms and two types of oxygen atoms: fivefold-coordinated Ti(5c), sixfold-coordinated Ti(6c), twofold-coordinated bridging O(2c), and threefold-coordinated in-plane O(3c). Here, we only considered a partially reduced surface which is gener-

a)Author to whom correspondence should be addressed. Fax: 512-471-7060. Electronic mail: gshwang@che.utexas.edu

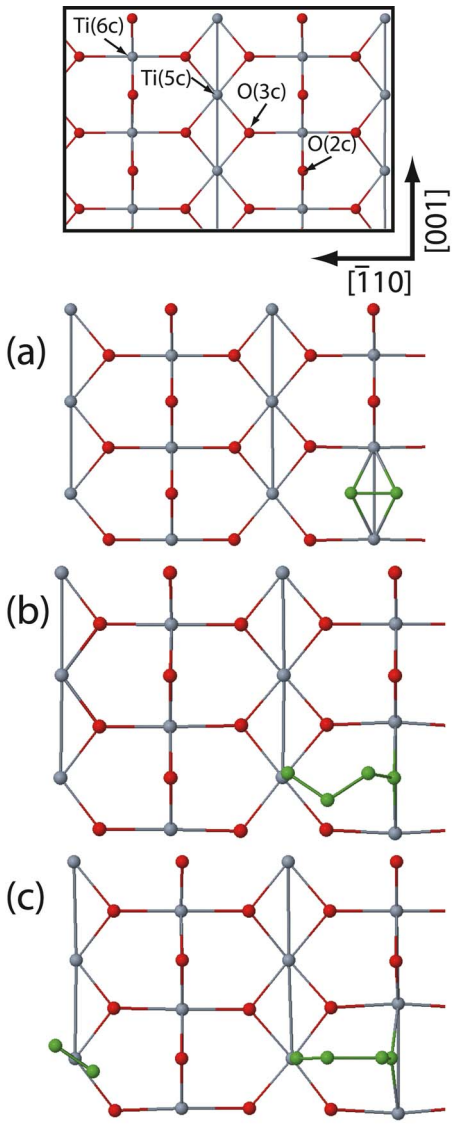

FIG. 1. (Color online) Top view of the lowest-energy configuration of molecularly adsorbed O_2 on reduced $TiO_2(110)$. (a) $\theta=1$, (b) $\theta=2$, and (c) $\theta=3$, where θ is defined as the number of O_2 per oxygen vacancy. The top view of the stoichiometric $TiO_2(110)$ surface is also shown. The green, red, and gray balls represent adsorbed O, surface O, and Ti atoms, respectively.

ated by removing a bridging O($2c$) atom from a given surface unit cell. Indeed, spin-polarized DFT calculations[18,21] have predicted that the formation of vacancy pairs or larger vacancy clusters would be energetically less favorable, relative to isolated vacancies, due to a repulsive vacancy-vacancy interaction. This is consistent with earlier scanning tunneling microscopy (STM) measurements demonstrating that the majority of oxygen vacancies remain isolated.[22]

A. O_2 adsorption

Electron delocalization from the vacancy site is likely to affect the adsorption of O_2 molecules. As mentioned earlier approximately three O_2 molecules can adsorb per oxygen vacancy on the reduced $TiO_2(110)$ surface.[6] These observations have alluded that in addition to oxygen vacancies, Ti($5c$) atoms can provide stable adsorption sites. This adsorption behavior of O_2 can be supported by results from a series of recent first principles density functional calculations which examined the interaction of O_2 molecules with the reduced TiO_2 surface.[10–12] Since the scope of this paper is to show the effect of O_2 coverage on the CO oxidation reaction, here we only discuss the lowest-energy configurations of adsorbed oxygen species at varying O_2 coverages ($\theta=1$, 2, and 3, where θ is defined as the number of O_2 per oxygen vacancy). The details of the adsorption properties of O_2 (in the absence of CO) at higher coverages ($\theta>1$) will be presented elsewhere.

At $\theta=1$, as shown in Fig. 1(a), the most favorable adsorption position is the vacancy site where O_2 is aligned in a parallel configuration. Our DFT generalized gradient approximation (GGA) calculation gives the O_2 adsorption energy of $E_{ad}=2.72$ eV,

$$E_{ads} = -E_{O_2TiO_2} + E_{TiO_2} + E_{O_2},$$

where E_{O_2/TiO_2}, E_{TiO_2}, and E_{O_2} refer to the total energies of the oxygen species adsorbed on the TiO_2 surface, the (stoichiometric or reduced) $TiO_2(110)$ surface, and an oxygen molecule in the gas phase, respectively.

The adsorption of O_2 along the neighboring Ti($5c$) row turns out to be 0.77–1.38 eV less favorable than in the vacancy position. The adsorbed O_2 is predicted to undergo diffusion along the Ti($5c$) row, with a barrier of 0.54 eV. In addition, the bond length of the vacancy-bound O_2 is elongated to 1.48 Å, close to 1.46 Å for O_2^{2-} in H_2O_2, suggesting that approximately two electrons transfer from the surface to the O_2 molecule.

At $\theta=2$, the tetraoxide complex across the O vacancy and an adjacent Ti($5c$) atom are predicted to be most energetically stable [Fig. 1(b)]. The O_4 binding energy is approximately 2.93 eV with respect to two isolated O_2 molecules in the gas phase. Our calculation predicts that the dissociation of O_4 into two separately adsorbed O_2, one in a parallel configuration above the vacancy site and the other diagonally adsorbed above the Ti($5c$) site, requires overcoming a barrier of approximately 1.25 eV. It appears that the dissociation process is endothermic by 0.90 eV, and the O_2 molecule at the Ti($5c$) site can easily desorb with a barrier of 0.30 eV.

The O–O bond lengths in the O_4 complex are 1.50, 1.42, and 1.55 Å, between O1–O2, O2–O3, and O3–O4, respectively, where O1 is the O atom at the vacancy site, O2 is the next nearest neighbor to the vacancy oxygen atom (O1), and O3 is between O2 and O4 [which is at the atop site above the neighboring Ti($5c$) atom]. Our results show that the atomic structure is close to that of gas-phase O_4^{2-} in H_2O_4 (which yields 1.50, 1.45, and 1.50 Å for corresponding O1–O2, O2–O3, and O3–O4, respectively). This gas-phase O_4^{2-} structure is in good agreement with previous high level singles doubles configuration interaction (CISD) theoretical results.[23] We attribute the small discrepancy between the adsorbed and gas-phase O_4 complexes to the geometric constraint that the reduced $TiO_2(110)$ surface imposes on the adsorbed O_4.

At $\theta=3$, as illustrated in Fig. 1(c), the most stable adsorption structure consists of a tetraoxide complex at the vacancy site and an additional oxygen molecule atop a Ti($5c$)

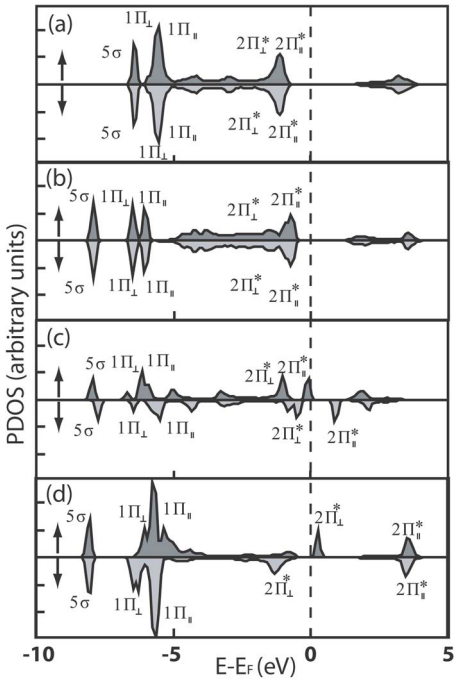

FIG. 2. Projected density of states (PDOS) spectra for spin up (↑) and spin down (↓) electrons of oxygen adspecies. (a) O_2 at the vacancy site when $\theta=1$, (b) O_4 at the vacancy site when $\theta=2$, (c) O_4 at the vacancy site when $\theta=3$, and (d) O_2 at the Ti($5c$) site when $\theta=3$. The dotted line indicates the Fermi level position.

atom in the neighboring row. The binding energy of the third O_2 is predicted to be 0.41 eV. The additional O_2 adsorption results in a noticeable change in the bonding configuration of O_4; that is, the O–O bond lengths become 1.35, 1.70, and 1.39 Å between O1–O2, O2–O3, and O3–O4, respectively. The atomic structure is virtually identical to that of a gas-phase O_4^- in HO_4 in which the corresponding O1–O2, O2–O3, and O3–O4 lengths are 1.32, 1.79, and 1.41 Å, respectively. The gas-phase O_4^- geometry agrees well with previous theoretical results.[24] We also find that the bond length of the O_2 above the Ti($5c$) atom is 1.39 Å, close to 1.37 Å for O_2^- in HO_2. The bond length variation is indicative of an electron transferring from the surface to each of the adsorbed O_2 and O_4 species.

Figure 2 shows the spectra of the local density of states (LDOS) projected on the adsorbed oxygen species, which demonstrates the activation of adsorbed O_2 molecules via charge transfer from the reduced TiO_2 surface. As shown in Figs. 2(a) and 2(b), the full spin manifold of the antibonding $2\pi^*$ states of O_2 (at $\theta=1$) and O_4 (at $\theta=2$) is located below the Fermi energy (E_F), indicating the filling of the antibonding orbitals that results in a strong activation of the oxygen species. On the other hand, at $\theta=3$, the LDOS spectra of O_2 and O_4 show that the O $2\pi^*$ bands shift significantly higher in energy, but the spin down $2\pi^*_\perp$ state is still slightly below E_F. This indicates that the activation of O_2^- and O_4^- species (at $\theta=3$) is attributed to occupation of the $2\pi^*_\perp$ orbital, albeit not as strong as when $\theta \leqslant 2$.

B. CO adsorption

The interaction of CO with the rutile TiO_2(110) surface is relatively well known, although there is still some controversy about the adsorption structure and energetics of CO on defective surfaces.[13,25,26] For the purpose of comparison, we also calculated the adsorption properties of CO on both stoichiometric and reduced surfaces.

On the stoichiometric surface the most stable adsorption site is above a Ti($5c$) atom with the C moiety of CO closest to the surface, as a well-known fact that CO usually binds to the cationic site of metal oxide surfaces.[25] Our DFT-GGA calculation gives the CO binding energy of 0.37 eV, in good agreement with other DFT results of approximately 0.37 eV (Refs. 13, 24, and 25) and experimental observations of about 0.43 eV.[1] All other binding sites considered along a bridging O($2c$) row with either the C or O moiety of CO closest to the surface have adsorption energies less than 0.10 eV, as also predicted by previous DFT studies.[25,26] Here, the CO adsorption energy is given as

$$E_{\text{ads}} = -E_{\text{CO-}(s/r)\text{TiO}_2} + E_{(s/r)\text{TiO}_2} + E_{\text{CO}},$$

where $E_{\text{CO-}(s/r)\text{TiO}_2}$, $E_{(s/r)\text{TiO}_2}$, and E_{CO} are the energies of CO adsorbed on the stoichiometric/reduced TiO_2 surface, stoichiometric/reduced TiO_2(110) surface, and the gas-phase CO molecule, respectively.

On the reduced surface, CO has been found to adsorb not only at the atop sites above Ti($5c$) atoms, but also at the O-vacancy site.[1] Thus, CO saturation coverage is likely to increase with the density of oxygen vacancies on reduced TiO_2(110). The CO binding energies at the Ti($5c$) and O-vacancy sites are respectively estimated to be 0.37 and 0.38 eV from our DFT-GGA calculations. Given the electron delocalization that occurs from the oxygen vacancy creation, we expect that CO adsorption involves some back donation of charge from the surface to the CO-π^* states, similar to the

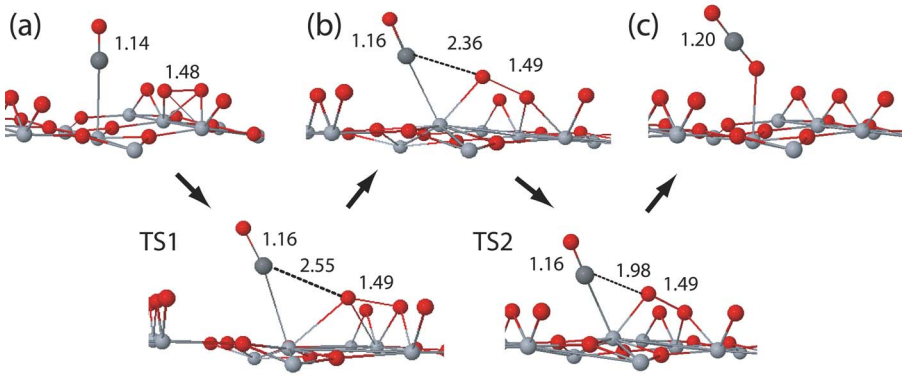

FIG. 3. (Color online) Reaction pathway (upper) and barrier (lower) for the reaction of CO with O_2 at the vacancy site when $\theta=1$. The red, gray, and dark gray balls represent O, Ti, and C atoms, respectively. All distances are given in Å and all energies are in eV.

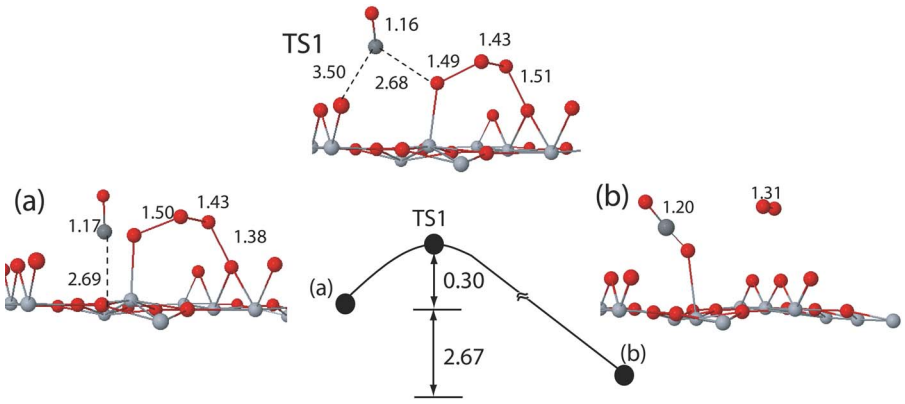

FIG. 4. (Color online) Reaction pathway (upper) and barrier (lower) for the reaction of CO with O_4 at the vacancy site when $\theta=2$. The red, gray, and dark gray balls represent O, Ti, and C atoms, respectively. All distances are given in Å and all energies are in eV.

bonding between CO and metal surfaces. The CO binding energies change slightly when another O vacancy is created on the (2×3) $TiO_2(110)$ surface, where two O vacancies are located in opposing oxygen rows diagonal to each other. This suggests that the presence of a moderate density of single O vacancies insignificantly alters the adsorption properties of CO on $TiO_2(110)$. Our results show that the inclusion of spin polarization has no effect on CO adsorption energy, and the spin state of the surface does not change with CO adsorption. The results are overall consistent with previous theoretical studies.[13,25,26]

While CO has been known to adsorb weakly on both reduced and oxidized TiO_2 surfaces, earlier experiments also observed an increase in adsorption strength with increasing surface reduction. In fact, previous DFT studies[13,26] have shown a large increase in adsorption energy to 1.16 eV atop the row vacancy sites, but not atop Ti(5*c*) sites. This could be attributed to a reduction in vacancy-vacancy repulsion upon CO adsorption as a result of the transfer of excess electrons available on the reduced surface to the CO-π^* states. Note that there exists a strong repulsion between two adjacent O vacancies.[18,21] We also determined that at room temperature CO may easily undergo diffusion along a Ti(5*c*) row with a moderate barrier of approximately 0.3 eV.

C. CO oxidation

Based on the adsorption structures of O_2 and CO molecules determined earlier, we examined the pathways and barriers for the reaction of CO with O_2 and O_4 species at $\theta=1-3$. The results are summarized in Figs. 3–6.

First, we looked at CO interaction with O_2 adsorbed horizontally at the vacancy site (when $\theta=1$, see Fig. 3). The CO molecule is initially placed at the atop site above a Ti(5*c*) atom adjacent to the O vacancy [(a)], yielding CO adsorption energy of 0.36 eV. Then, the horizontal O_2 is allowed to reconfigure to the tilted O_2 position, which requires overcoming a barrier of 0.45 eV [(b)]. The tilted configuration is about 0.20 eV less favorable than the horizontal configuration, yielding a return barrier of approximately 0.25 eV. Note that the energy difference between the horizontal and tilted configurations reduces to 0.15 eV and the transformation barrier is 0.35 eV when there is no CO present.[11] Once in the tilted position CO can easily interact with the adsorbed O_2 and form CO_2 with a barrier of 0.22 eV. This reaction is exothermic by 3.95 eV. Under the steady-state approximation, the overall barrier is estimated to be 0.45 eV, in good agreement with 0.4 eV from previous DFT studies.[13]

Next, as illustrated in Fig. 4, we determined a pathway for CO reaction with O_4 at the vacancy site when $\theta=2$. When CO is placed at the site between the O4 atom and the neighboring bridging O(2*c*) atom [(a)], it reacts with the highly active O_4 complex with no sizable barrier. This reaction is also exothermic by 2.67 eV. The oxidation process results in O_4 dissociation into an O atom which heals the vacancy, and an O_2 molecule which desorbs [(b)]. Given the weak interaction of CO with the TiO_2 surface, we can expect that CO molecules may roam across the surface (with a barrier of approximately 0.3 eV as predicted earlier) and easily react with O_4 complexes even at room temperature when the O_2 coverage is sufficiently low, i.e., $\theta\leqslant2$.

Finally, we considered the reaction of CO with O_4 at the vacancy site when $\theta=3$ (see Fig. 5). Since CO can diffuse with a barrier of around 0.3 eV along the Ti row to the site between the bridging oxygen and O4 atom, we begin with the local minimum structure as shown in Fig. 5(a). Then, the

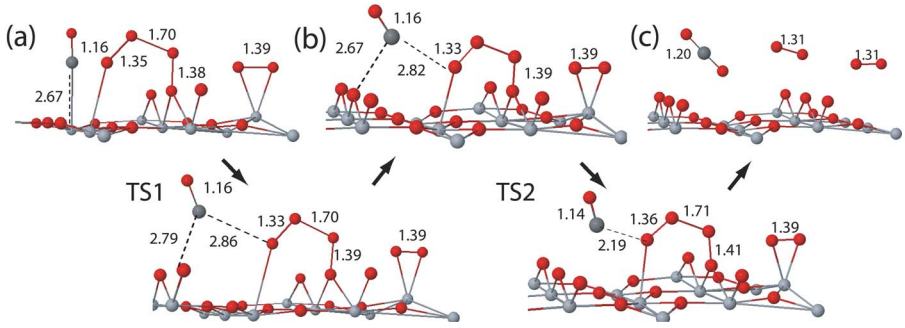

FIG. 5. (Color online) Reaction pathway (upper) and barrier (lower) for the reaction of CO with O_4 at the vacancy site when $\theta=3$. The red, gray, and dark gray balls represent O, Ti, and C atoms, respectively. All distances are given in Å and all energies are in eV.

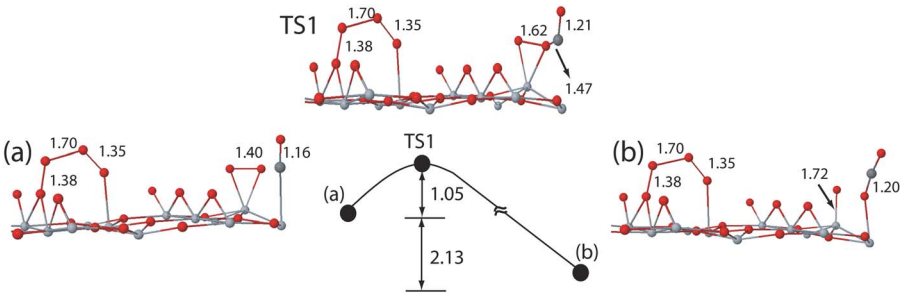

FIG. 6. (Color online) Reaction pathway (upper) and barrier (lower) for the reaction of CO with O_2 at the Ti(5*c*) site when θ=3. The red, gray, and dark gray balls represent O, Ti, and C atoms, respectively. All distances are given in Å and all energies are in eV.

CO molecule is allowed to react with the O_4 complex to form CO_2. This oxidation process is predicted to occur by overcoming a sizable barrier of 0.70 eV, contrary to nearly no barrier when θ=2. This indicates that the reactivity of oxygen species towards CO oxidation significantly varies with the degree of reoxidation of TiO_2(110). For the sake of completeness, we also considered CO oxidation occurring with the O_2 molecule adsorbed above the Ti(5*c*) site (see Fig. 6). The energy barrier for this reaction is predicted to be greater than 1 eV, suggesting that the O_2 molecule may preferably undergo desorption rather than reaction with coadsorbed CO to form CO_2, given the much smaller desorption energy (≈0.4 eV).

Our results clearly demonstrate that there is a strong O_2-coverage dependence of the activation energy for CO oxidation on TiO_2(110). We also suspect that, to some degree, the coverage-dependent behavior may be responsible for the reactivity change of O_2 towards photoinduced CO oxidation as reported by Lu *et al.*[9] According to their experimental observations, oxygen adsorption at 105 K produces primarily the α state which is thermally converted to the β state upon heating TiO_2 above 200 K. Heating the surface will result in O_2 desorption and/or O_2 dissociation. The process of O_2 dissociation can annihilate oxygen vacancies, which may in turn alter the amount of oxygen species per vacancy. To understand the complex surface reactions, further theoretical studies of photoinduced desorption of and CO oxidation by O_2 and O_4 species at various charge states are necessary.

IV. SUMMARY

Based on density functional slab calculations we examined the effect of varying O_2 coverage on the CO oxidation reaction on reduced rutile TiO_2(110) surfaces. First, we determined lowest-energy configurations of oxygen adspecies by varying the number of adsorbed O_2 molecules per vacancy (θ=1–3) as well as the adsorption properties of CO on both stoichiometric and reduced surfaces. Our results show the existence of O_2 and O_4 species at various charge states; that is, $O_2^{2-}(\theta=1)$, $O_4^{2-}(\theta=2)$, $O_2^{-}(\theta=3)$, and $O_4^{-}(\theta=3)$. In addition, CO adsorption is found to occur at both the O-vacancy site and the atop sites above Ti(5*c*) atoms with a binding energy of 0.37–0.38 eV. Adsorbed CO is also predicted to undergo diffusion along a Ti(5*c*) row with a barrier of about 0.3 eV, until it desorbs or reacts with oxygen adspecies to form CO_2. Overall activation energies of 0.45 and ≈0 eV are predicted, respectively, for reaction of CO with $O_2^{2-}(\theta=1)$ and $O_4^{2-}(\theta=2)$, whereas they appear to significantly increase to 0.7 and >1.0 eV, respectively, for O_4^{-} and O_2^{-} at θ=3. However, given its smaller desorption energy of ≈0.4 eV, the third O_2^{-} molecule (at θ=3) may preferably desorb, rather than react with coadsorbed CO. As such, at room temperature we can expect that oxygen adspecies may mostly exist in the form of O_2^{2-} or O_4^{2-} at the vacancy site, thereby giving an activation energy of less than 0.45 eV for CO oxidation. These results suggest the occurrence of room-temperature CO oxidation on O_2-predosed TiO_2(110), consistent with recent experiments reported by Lee *et al.*[7] We also suspect that, to some degree, the coverage-dependent behavior may be responsible for the reactivity change of O_2 towards photoinduced CO oxidation as reported by Yates and co-workers,[8,9] considering that heating the surface will alter the amount of oxygen species per vacancy by O_2 desorption and vacancy annihilation from O_2 dissociation. A clear understanding of the complex surface processes requires further studies of photoinduced desorption of and CO oxidation by these oxygen adspecies at various charge states.

ACKNOWLEDGMENTS

This work was supported by the Welch Foundation (Grant No. F-1535). One of the authors (G.S.H.) also thanks the NSF (CAREER-CTS-0449373 and ECS-0304026) for the partial financial support. All the calculations were performed using supercomputers in Texas Advanced Computing Center at the University of Texas at Austin.

[1] A. Linsebigler, G. Q. Lu, and J. T. Yates, J. Chem. Phys. **103**, 9438 (1995).
[2] *Sensors*, edited by A. Gopel, J. Hesse, and J. N. Zemel (VCH, Weinheim, 1989).
[3] C. R. Henry, Surf. Sci. Rep. **31**, 1998235 (1998).
[4] M. Valden, X. Lai, and D. W. Goodman, Science **281**, 1647 (1998).
[5] C. T. Campbell, S. C. Parker, and D. E. Starr, Science **298**, 811 (2002).
[6] M. A. Henderson, W. S. Epling, C. L. Perkins, C. H. F. Peden, and U. Diebold, J. Phys. Chem. B **103**, 5328 (1999).
[7] S. S. Lee, C. Y. Fan, T. P. Wu, and S. L. Anderson, J. Am. Chem. Soc. **126**, 5682 (2004).
[8] G. Q. Lu, A. Linsebigler, and J. T. Yates, J. Chem. Phys. **102**, 4657 (1995).
[9] G. Q. Lu, A. Linsebigler, and J. T. Yates, J. Chem. Phys. **102**, 3005 (1995).
[10] M. D. Rasmussen, L. M. Molina, and B. Hammer, J. Chem. Phys. **120**, 988 (2004).
[11] Y. Wang, D. Pillay, and G. S. Hwang, Phys. Rev. B **70**, 193410 (2004).
[12] X. Y. Wu, A. Selloni, M. Lazzeri, and S. K. Nayak, Phys. Rev. B **68**, 241402 (2003).
[13] X. Y. Wu, A. Selloni, and S. K. Nayak, J. Chem. Phys. **120**, 4512 (2004).
[14] J. P. Perdew, J. A. Chevary, S. H. Vosko, K. A. Jackson, M. R. Pederson, D. J. Singh, and C. Fiolhais, Phys. Rev. B **46**, 6671 (1992).

[15] G. Kresse and J. Hafner, Phys. Rev. B **47**, 558 (1993).
[16] D. Pillay and G. S. Hwang, Phys. Rev. B **72**, 205422 (2005).
[17] D. Pillay, Y. Wang, and G. S. Hwang, Catal. Today **105**, 78 (2005).
[18] D. Pillay, Y. Wang, and G. S. Hwang, Korean J. Chem. Eng. **21**, 537 (2004).
[19] D. Pillay and G. S. Hwang, J. Mol. Struct. **771**, 129 (2006).
[20] G. Henkelman and H. Jonsson, J. Chem. Phys. **113**, 9978 (2000).
[21] A. Vijay, G. Mills, and H. Metiu, J. Chem. Phys. **118**, 6536 (2003).
[22] U. Diebold, J. Lehman, T. Mahmoud, M. Kuhn, G. Leonardelli, W. Hebenstreit, M. Schmid, and P. Varga, Surf. Sci. **411**, 137 (1998).
[23] J. T. Fermann, B. C. Hoffman, G. S. Tschumper, and H. F. Schaefer, J. Chem. Phys. **106**, 5102 (1997).
[24] G. V. Chertihin and L. Andrews, J. Chem. Phys. **108**, 6404 (1998).
[25] M. Menetrey, A. Markovits, and C. Minot, Surf. Sci. **524**, 49 (2003).
[26] D. C. Sorescu and J. T. Yates, J. Phys. Chem. B **106**, 6184 (2002).